Supplementary Information (SI) for Journal of Materials Chemistry A.

Supporting Information for

Engineering Compressive Strain in Pd through Surface Reconstruction of Ag_2Se for Enhanced Formate Oxidation

Zhen Li,[ab] Fuyi Chen,*[ab] Junpeng Wang,[ab] Chongyang Wang,[ab] Shuang Shan[ab] and Longfei Guo[ab]

a.State Key Laboratory of Solidification Processing, Northwestern Polytechnical University, Xi'an 710072, China. E-mail: fuyichen@nwpu.edu.cn
b.School of Materials Science and Engineering, Northwestern Polytechnical University, Xi'an, 710072, China

Corresponding author at: State Key Laboratory of Solidification Processing, Northwestern Polytechnical University, Xi'an 710072, China.
E-mail address: fuyichen@nwpu.edu.cn.

Table S1 Example of tunable strain induced by volume manipulation.

Catalyst	Reference
Pt-Li battery	1
Pd-P@Pt	2
Pd-H@Pt	3
PtMnCo	4
PdN	5

Table S2 Electrocatalytic Performance Comparison for the Formate Oxidation Reaction (FOR) in Alkaline Media.

Catalyst	Electrolyte	Mass activity (A/mgPd)	Durability remain at 3600s in CA	Reference
Ag_2Se-Pd	1 M KOH+ 1 M HCOOK	3.59	46%	This work
PdH	1 M KOH+0.5 M HCOOK	0.85	20%	6
PdCu/C	1 M KOH+ 1 M HCOOK	2.0	14%	7
PdP/WO3	1 M KOH+1 M HCOOK	0.50	--	8
AgPdCu	1 M KOH+1 M HCOOK	2.73	16%	9
PdRh/C	1 M KOH+1 M	4.50	17%	10

	HCOOK			
PdCe/C	1 M KOH+ 1 M HCOOK	1.10	10%	11
Pd@PdPt	1 M KOH + 0.5 M HCOOK	1.25	20%	12
AgPt	1 M KOH + 0.5 M HCOOK	0.38	55%	13
AuAgPd	1 M KOH+1 M HCOOK	4.51	29%	14
AgPdRh	1 M KOH+1 M HCOOK	1.85	10%	15
PdPt	1 M KOH+0.5 M HCOOK	1.65	20%	16
Pd/FeOx/C	1 M KOH+1 M HCOOK	1.61	--	17

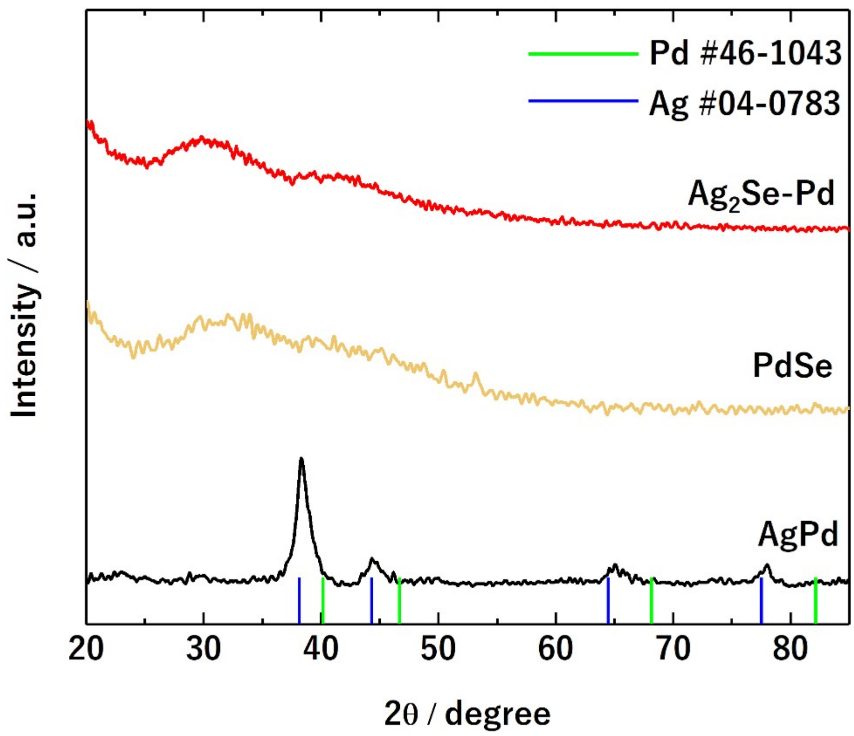

Figure S1. X-ray diffraction (XRD) patterns of Ag_2Se–Pd, PdSe, and conventional AgPd nanoparticles.

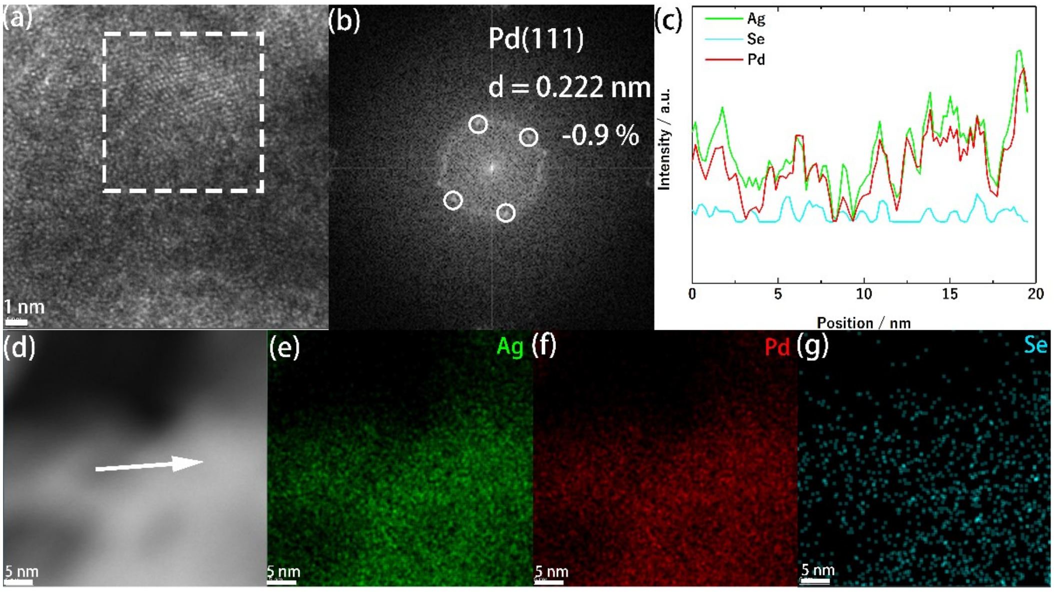

Figure S2. TEM characterization of the residual Ag_2Se–Pd catalyst after the chronoamperometry (CA) test. (a) HRTEM image. (b) FFT pattern of the white square region in (a). (c) EDS line scan along the arrow shown in the HAADF image (d). (d) HAADF-STEM image. (e–g) EDS elemental maps of the region shown in (d).

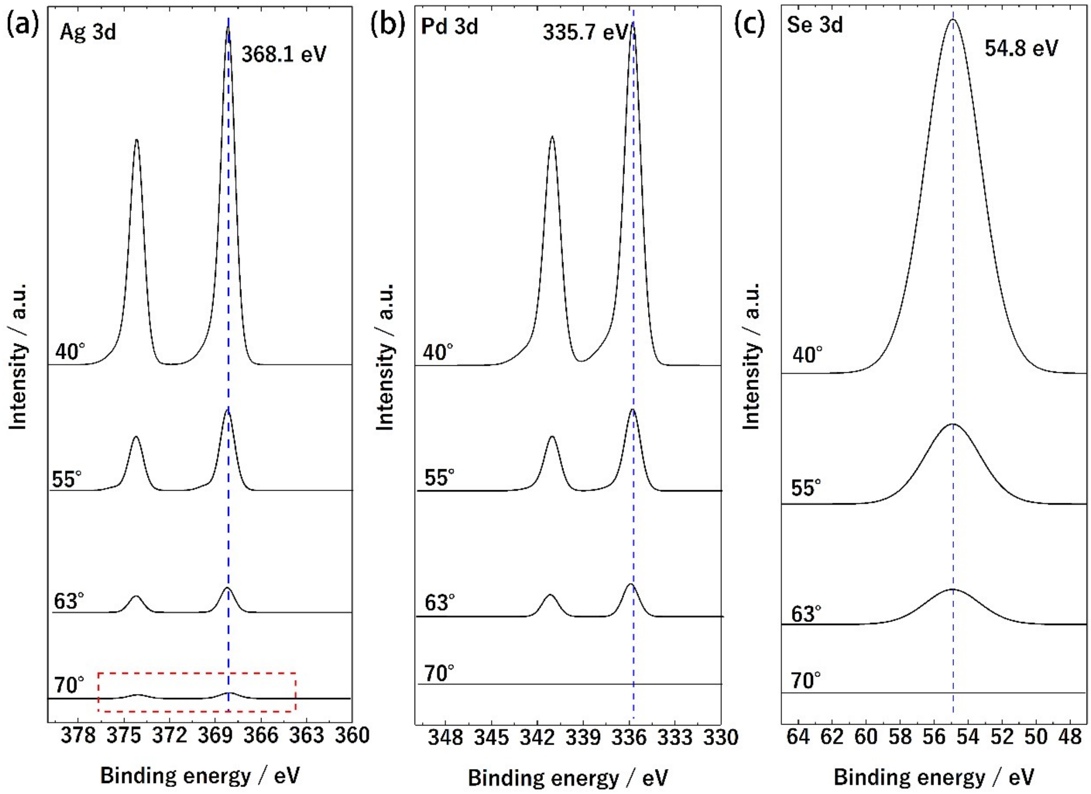

Figure S3. Angle-resolved XPS spectra of the as-prepared Ag_2Se–Pd: (a) Ag 3d, (b) Pd 3d, and (c) Se 3d.

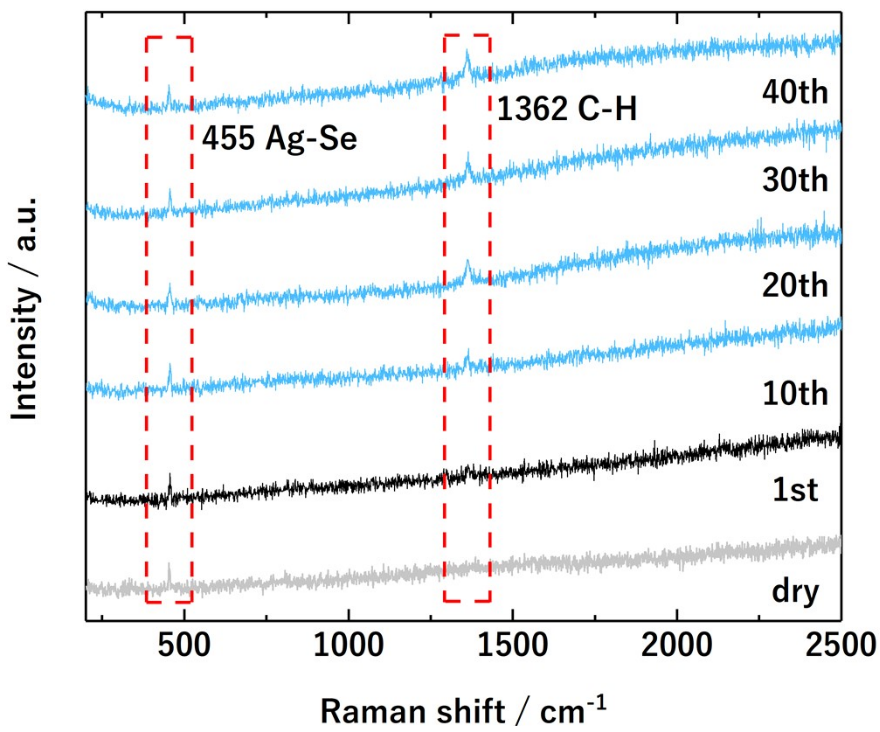

Figure S4. In situ Raman spectroscopy of Ag_2Se–Pd during electrochemical activation. The measurements were performed in 1 M KOH + 1 M HCOOK electrolyte (pH = 14) with an upper potential limit of 1.13 V vs. RHE.

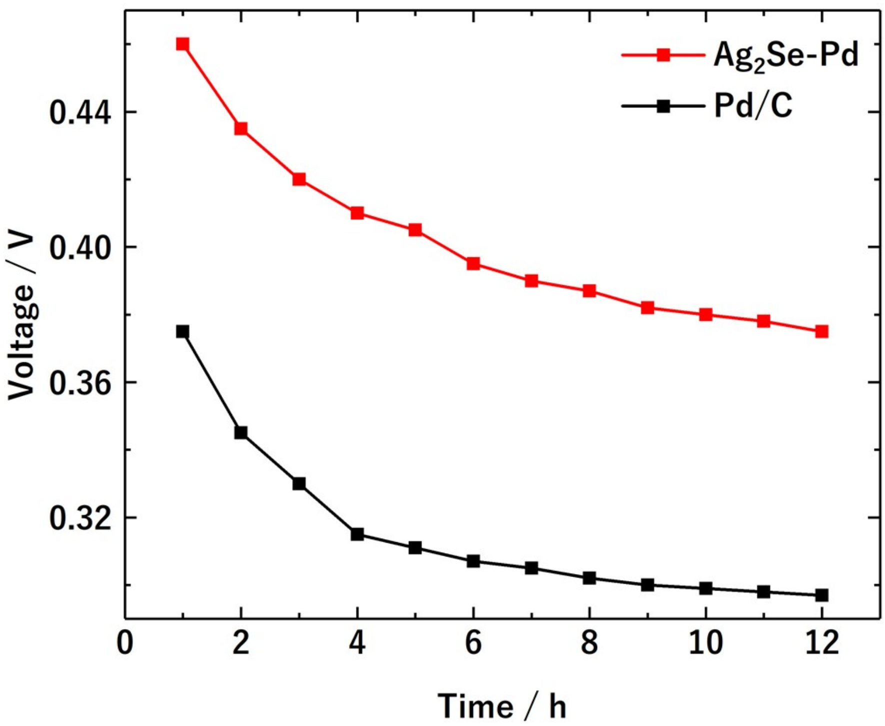

Figure S5. Galvanostatic voltage decay test of the DFFC. The fuel cell was operated with an electrolyte flow of 0.5 mL min^{-1} (1 M HCOOK + 1 M KOH) and an O_2 flow of 100 sccm, at a constant current density of 100 mA cm^{-2}.

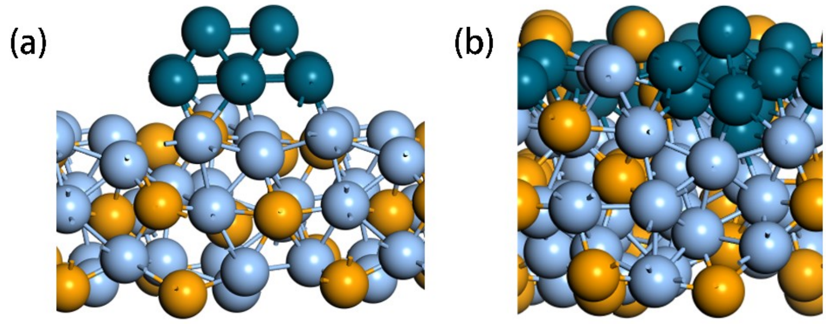

Figure S6. Structural models of Ag_2Se–Pd before and after geometric optimization. (a) Initial configuration: a Pd_{13} cluster placed on the Ag_2Se(112) surface prior to relaxation. (b) Optimized structure after full geometric relaxation, showing partial embedding of the Pd cluster into the Ag_2Se substrate and the resulting amorphous character, consistent with experimental observations.

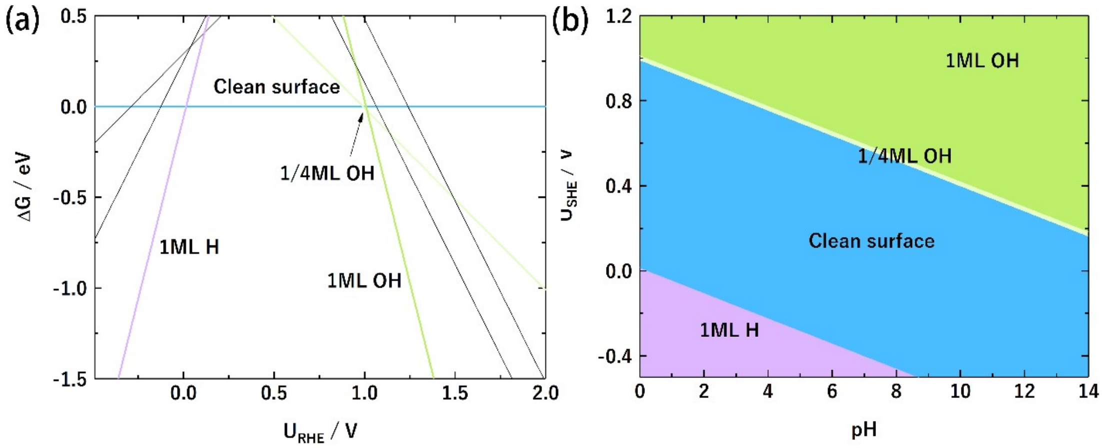

Figure S7. (a) Surface phase diagram and (b) Pourbaix diagram of Ag_2Se–Pd.

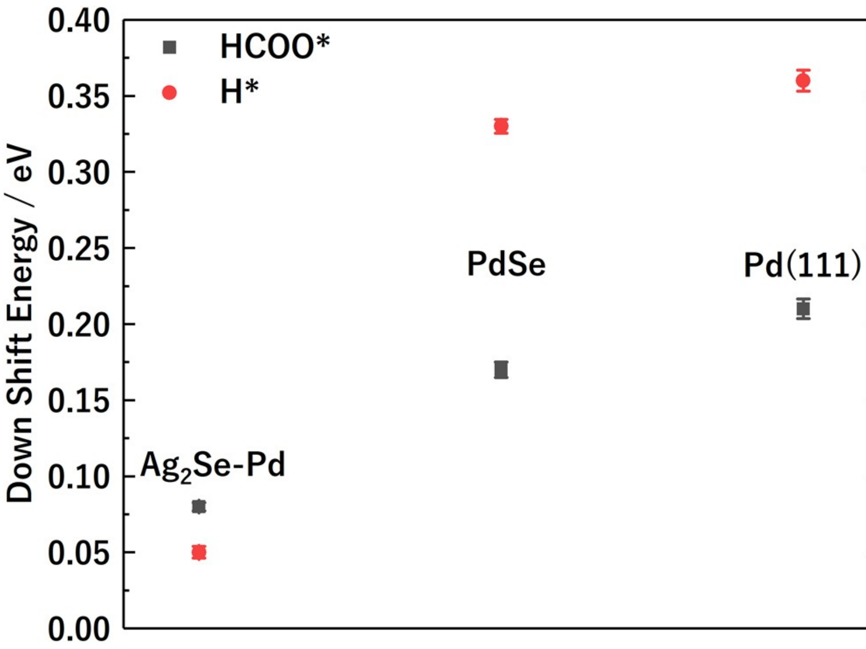

Figure S8. Bar chart with error bars showing the changes in the d-band center of Pd upon adsorption of HCOO* and H*.

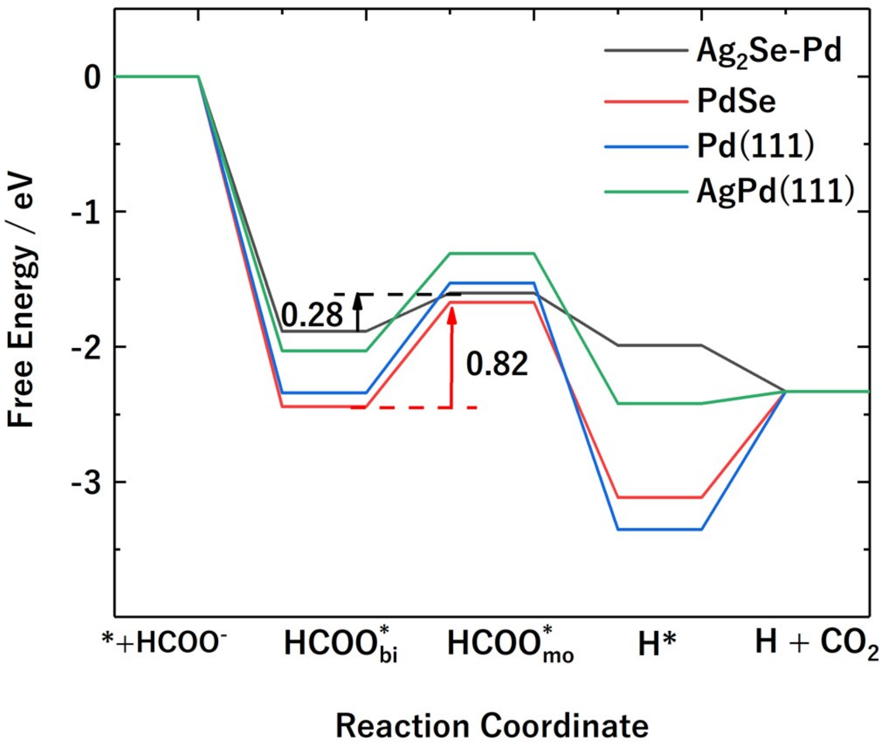

Figure S9. Free energy diagram of the formate oxidation reaction (FOR) pathway.

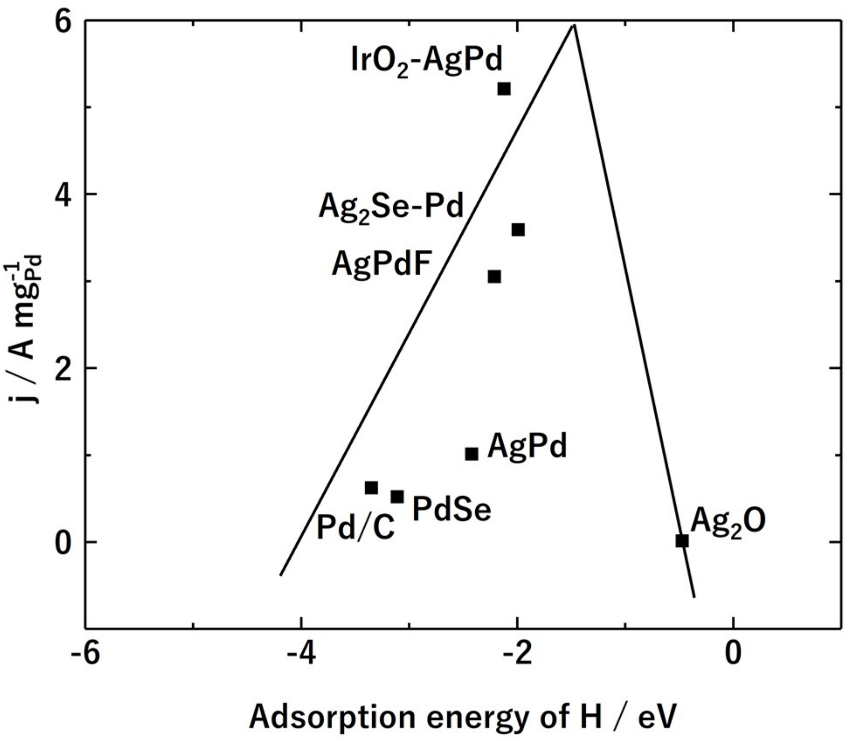

Figure S10. Volcano plot of FOR mass activity as a function of H* adsorption energy.

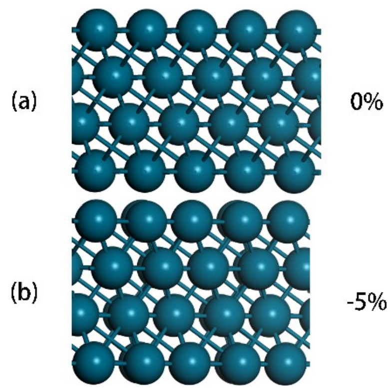

Figure S11. Side views of the Pd(111) slab models used for strain-dependent DFT calculations. (a) Unstrained Pd(111) surface with the equilibrium lattice constant. (b) Pd(111) surface under -5% biaxial compressive strain applied in the lateral directions.

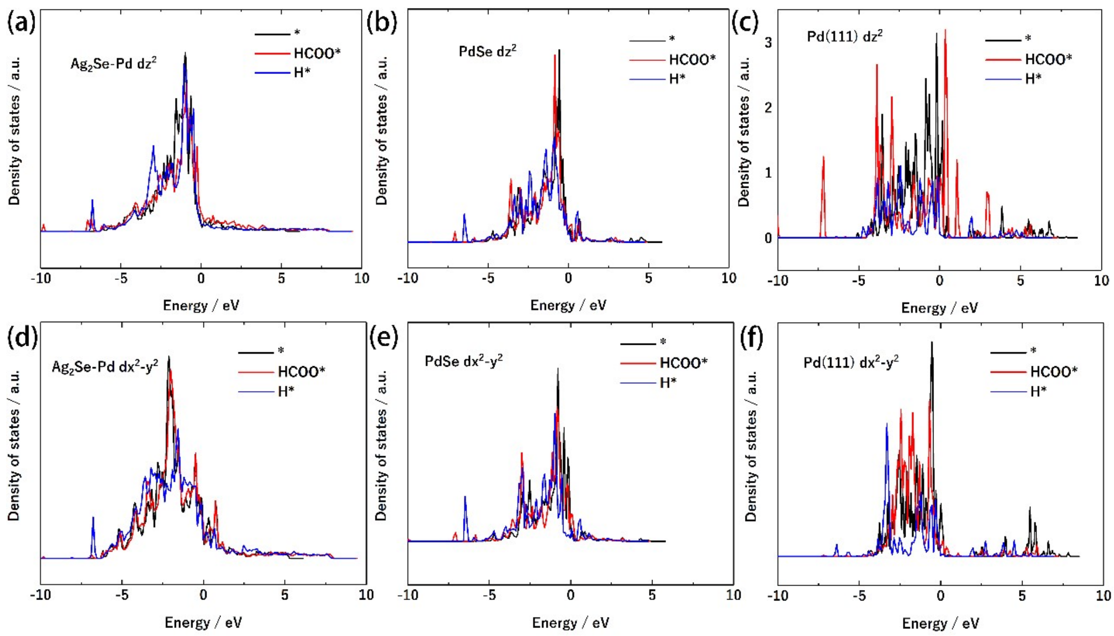

Figure S12. Density of states (DOS) plots of the (a–c) dz^2 and (d–f) dx^2-y^2 orbitals of Pd on the Ag_2Se–Pd, PdSe, and Pd(111) surfaces during the FOR steps.

References

1. H. Wang, S. Xu, C. Tsai, Y. Li, C. Liu, J. Zhao, Y. Liu, H. Yuan, F. Abild-Pedersen, F. B. Prinz, J. K. Nørskov and Y. Cui, Science, 2016, 354, 1031-1036.

2. T. He, W. Wang, F. Shi, X. Yang, X. Li, J. Wu, Y. Yin and M. Jin, Nature, 2021, 598, 76-81.

3. G. Liu, W. Zhou, Y. Ji, B. Chen, G. Fu, Q. Yun, S. Chen, Y. Lin, P.-F. Yin, X. Cui, J. Liu, F. Meng, Q. Zhang, L. Song, L. Gu and H. Zhang, Journal of the American Chemical Society, 2021, 143, 11262-11270.

4. M. Song, G. Luo, Q. Zhang, H. Hu and D. Wang, Science China Chemistry, 2025, 68, 536-542.

5. R. Guo, K. Zhang, Y. Liu, Y. He, C. Wu and M. Jin, Journal of Materials Chemistry A, 2021, 9, 6196-6204.

6. H.-Y. Sun, Y. Ding, Y.-Q. Yue, Q. Xue, F.-M. Li, J.-X. Jiang, P. Chen and Y. Chen, ACS Applied Materials & Interfaces, 2021, 13, 13149-13157.

7. W. J. Wang, S. Hwang, T. Kim, S. Ha and L. Scudiero, Electrochimica Acta, 2021, 387, 138531.

8. S. Kumar, R. Soni and S. Kurungot, Sustainable Energy & Fuels, 2021, 5, 4758-4770.

9. Q. Wang, F. Chen, L. Guo, T. Jin, H. Liu, X. Wang, X. Gong and Y. Liu, Journal of Materials Chemistry A, 2019, 7, 16122-16135.

10. J. Bai, Q. Xue, Y. Zhao, J.-X. Jiang, J.-H. Zeng, S.-B. Yin and Y. Chen, ACS Sustainable Chemistry & Engineering, 2019, 7, 2830-2836.

11. Q. Tang, F. Chen, T. Jin, L. Guo, Q. Wang and H. Liu, Journal of Materials Chemistry A, 2019, 7, 22996-23007.

12. Y.-C. Jiang, Y. Ding, F.-M. Li, S.-B. Yin, D.-S. Li, X.-F. Li and Y. Chen, Journal of Materials Chemistry A, 2022, 10, 24701-24707.

13. S.-H. Han, H.-M. Liu, J. Bai, X. L. Tian, B. Y. Xia, J.-H. Zeng, J.-X. Jiang and Y. Chen, ACS Applied Energy Materials, 2018, 1, 1252-1258.

14. B. Pan, F. Chen, B. Kou, J. Wang, Q. Tang, L. Guo, Q. Wang, Z. Li, W. Bian and J. Wang, Nanoscale, 2020, 12, 11659-11671.

15. Y. Jin, F. Chen, L. Guo, J. Wang, B. Kou, T. Jin and H. Liu, ACS Applied Materials & Interfaces, 2020, 12, 26694-26703.

16. X.-L. Liu, Y.-C. Jiang, J.-T. Huang, W. Zhong, B. He, P.-J. Jin and Y. Chen, Carbon Energy, 2023, 5, e367.

17. Y. Li, K. Zhang, Y. Ji, Z. Tang, Y. Yao, X. Liu, D. Wang, X. Wang, L. Shi, K. Nie, Z. Yang, J. Xie and Y.-M. Yan, ACS Applied Materials & Interfaces, 2023, 15, 28790-28798.